Materials Transactions, Vol. 49, No. 6 (2008) pp. 1456 to 1461

Polarization Behavior of Pure Magnesium under a Controlled Flow in a NaCl Solution

Sachiko Hiromoto[1,*], Akiko Yamamoto[1], Norio Maruyama[1], Hidetoshi Somekawa[2] and Toshiji Mukai[2]

[1]*Biometal Group, Biomaterials Center, National Institute for Materials Science, Tsukuba 305-0044, Japan*
[2]*Lightweight Alloys Group, Structural Metals Center, National Institute for Materials Science, Tsukuba 305-0047, Japan*

Magnesium and its alloys are potential candidates for bioabsorbable stents. The degradation rate of an indwelled magnesium stent is expected to be controlled under a blood flow. The influence of the controlled flow on the polarization and impedance behavior of pure Mg was thus investigated in a 0.6 mass% NaCl solution using a rotating electrode. The existence of a flow caused an increase in the anodic current density as well as a decrease in the impedance for a few hours of immersion, indicating the acceleration of Mg dissolution and the retardation of the growth of the surface hydroxide film. Interestingly, the existence of a flow retarded the breakdown of the surface film. After the surface film was broken down, the impedance did not depend on the rotation speed. To precisely evaluate the degradation rate of magnesium and its alloys for use in stents, the flow rate of the test solution should be controlled. [doi:10.2320/matertrans.MRA2008011]

(Received January 8, 2008; Accepted March 24, 2008; Published May 14, 2008)

Keywords: *pure magnesium, controlled flow, polarization behavior, impedance behavior, biomaterial*

1. Introduction

Magnesium and its alloys are candidates for bioabsorbable metals because a high concentration of magnesium is present as an essential element in the human body[1)] and magnesium is easily corroded in a physiological solution. The first attempts of the application of magnesium alloys for implant devices failed due to the formation of a hydrogen gas cavity around the implant devices. Hydrogen gas was generated accompanying by the corrosion of magnesium.[2–4)] The failure of these attempts was ascribed to the uncontrolled and very low corrosion resistance of the alloys. Since then, the corrosion resistance of magnesium alloys has been improved not only by alloying with aluminum and/or rare-earth elements but also by eliminating the contaminated elements, such as iron, nickel, and copper, which cause severe corrosion with a slight amount of contamination.[5)] The corrosion (degradation) rate of bioabsorbable metals must be controlled depending on the implanted part of the body and the kind of devices.

Recently, the application of commercial magnesium alloys (AE21[6,7)] and WE43[8,9)]) for bioabsorbable stents has been attempted, and some successful results have been obtained in clinical trials. The success of clinical trials is attributed to the relatively high corrosion resistance of the alloys. In addition, the rapid blood flow on the surface of an indwelled stent may have also contributed to the success because the blood flow accelerates mass diffusion, probably preventing the formation of a gas cavity and the pH change of blood near the surface of the stent while accelerating the dissolution of the magnesium alloy. The influence of the existence of a flow on the corrosion behavior of a magnesium alloy is reported in the following.[10–12)] The stirring of the carbonate buffer solution accelerated the corrosion of magnesium.[11)] Witte *et al.* suggested that the natural convection flow of body fluid around the implanted magnesium alloy caused the faster corrosion rate of AZ91D and LAE442 *in vivo* than that *in vitro*.[10)] The natural convection is derived by the surrounding blood flow. The blood flow rate varies from 0.1 to 1.0 m s^{-1} depending on the diameter of the blood vessel.[13,14)] Therefore, the influence of the existence of a flow on the corrosion behavior of a magnesium alloy should be elucidated to control the degradation rate of a magnesium device.

In this study, the influence of the controlled flow on the polarization and impedance behavior of pure magnesium is examined. The controlled flow was derived by rotating a magnesium disk electrode.

2. Experimental

2.1 Materials and electrolytes

A disk of pure Mg extrusion (99.9*% purity, Osaka Fuji Kogyo Co.) with a diameter of 8 mm and a thickness of 2 mm was used as a specimen. The measurements were carried out on a plane perpendicular to the direction of extrusion. The chemical composition of the pure Mg disk is shown in Table 1. The microstructure of the surface of the Mg disk was observed with an optical microscope. The Mg disk was fixed to an electrode holder of a rotating disk electrode (PAR). The surface of the Mg disk electrode was polished with #600 SiC polishing paper in ethanol, and the Mg disk was rinsed in acetone with an ultrasonic bath. Immediately after polishing, the Mg disk electrode was fixed onto a rotating shaft, and the rotation of the Mg disk electrode was started. The rotation speed was controlled at 0, 120, 240, 720, and 1440 rpm. The surface flow rate derived at 1440 rpm corresponds to 1 m s^{-1}, which is the maximum blood flow rate in the coronary artery. The rotating Mg disk electrode was immersed in an aerated 0.6% NaCl solution previously warmed at 310 K, and electrochemical measurements were carried out. The pH of the 0.6% NaCl solution was about 6 before using in the experiments, and no significant change in pH was observed after the experiments. The 0.6% NaCl solution was employed to make the Cl^- ion concentration of the solution equivalent

*Corresponding author, E-mail: HIROMOTO.Sachiko@nims.go.jp

Table 1 Chemical composition of Mg disk.

mass%	Al	Zn	Mn	Ni	Cu	Fe	Si	Pb	Ca	Sn	Cd	Mg
Mg	0.003	0.008	0.0037	0.0005	0.0003	0.0030	0.005	0.001	0.001	<0.001	<0.0001	Bal.

to that of blood plasma because the corrosion rate of pure Mg is very sensitive to the Cl^- ion concentration. In the polarization test of pure Mg as a preparatory experiment, the anodic current density around the corrosion potential of pure Mg in a 0.9% NaCl solution was 1.5 times higher than that in a 0.6% NaCl solution.

2.2 Electrochemical measurements

Open-circuit potential (ocp) and polarization measurements of the rotating Mg disk electrode were carried out in the NaCl solution at rotation speeds between 0 and 1440 rpm. The ocp of the rotating Mg disk electrode was monitored for 3.6 ks; subsequently, the potential was swept anodically and cathodically at a rate of 1 mV/s.

Impedance measurements were carried out on the rotating Mg disk electrode in the NaCl solution at immersion times of 0, 1.8, 3.6, 7.2, 14.4, and 21.6 ks. The rotation speed of the Mg disk electrode was controlled at 0 or 1440 rpm. The ac frequency ranged from 10^5 to 10^{-2} Hz with a sampling step of 12 points per decade. The polarization amplitude was 5 mV around the ocp.

A saturated calomel electrode (SCE) was used as the reference electrode, and a Pt wire loop was used as the counter electrode in all the measurements. The electrochemical measurements in this study were carried out using an ALS 660a electrochemical analyzer.

3. Results and Discussion

3.1 Microstructure

The typical microstructure of the pure Mg extrusion is shown in Fig. 1. No defect and inclusion were observed. The grain size was distributed from 30 to 200 μm. The average grain size was 60 μm.

3.2 ocp

Figure 2 shows the ocp transient curves of the Mg disk in the 0.6% NaCl solution at various rotation speeds. Figure 3 shows the optical surface images of the Mg disk immersed in the 0.6% NaCl solution for 3.6 ks at various rotation speeds. The ocp increased in the initial 300 s and showed a constant value that decreased with the increase of the rotation speed. In the cases of 0 and 120 rpm, the ocp increased in the last 600 s of immersion.

The corrosion of magnesium in a neutral solution proceeds as follows:[15,16]

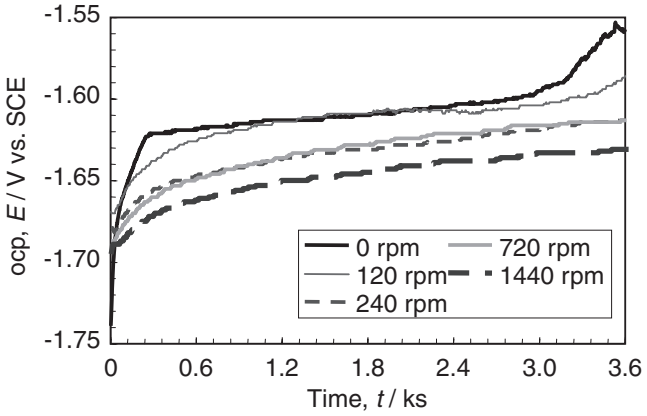

Fig. 2 ocp transient curves of a Mg disk at various rotation speeds in a 0.6% NaCl solution.

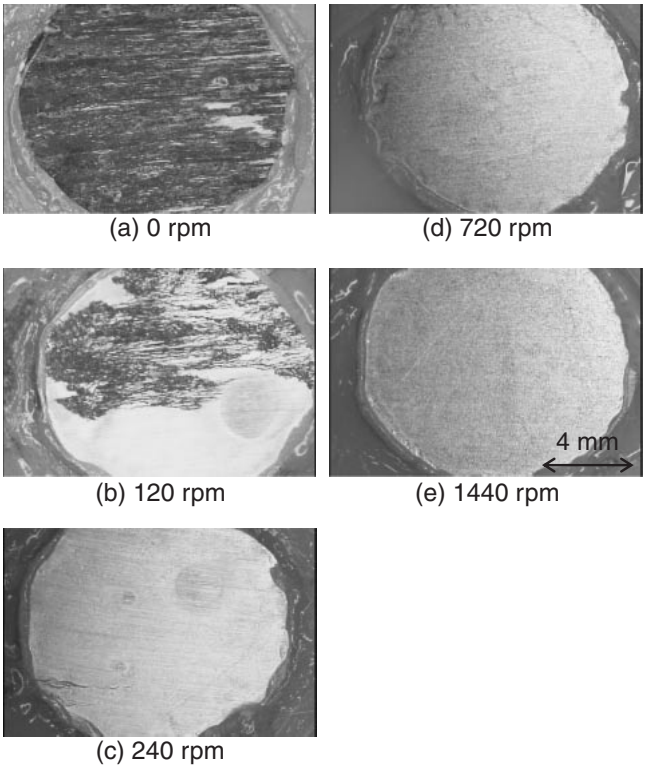

Fig. 3 Images of the surface of a Mg disk immersed for 3.6 ks in a 0.6% NaCl solution at (a) 0 rpm, (b) 120 rpm, (c) 240 rpm, (d) 720 rpm, and (e) 1440 rpm.

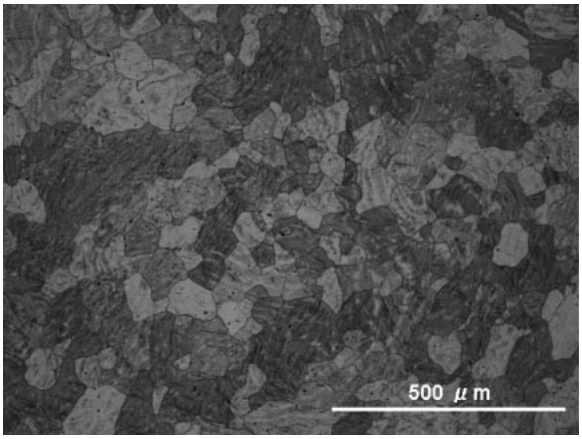

Fig. 1 Microstructure of a Mg disk on a plane perpendicular to the direction of extrusion.

$$Mg \rightarrow Mg^{2+} + 2e^- \quad (1)$$

$$2H_2O + 2e^- \rightarrow H_2 + 2OH^- \quad (2)$$

$$Mg^{2+} + 2OH^- \rightarrow Mg(OH)_2 \quad (3)$$

The pH of a solution increases with the generation of H_2 gas and OH^- ions, as shown in eq. (2). Then, $Mg(OH)_2$ is formed on the surface of magnesium, as shown in eq. (3), because $Mg(OH)_2$ is stable at around room temperature.[16] Beside the above electrochemical corrosion reaction, the chemical dissolution of $Mg(OH)_2$ may have simultaneously taken place in the 0.6% NaCl solution.[16,17]

The initial increase of ocp is owing to the growth of the $Mg(OH)_2$ film, which rapidly takes place immediately after immersing magnesium in the neutral solutions.[17] The decrease of the constant ocp with the increase of the rotation speed is attributed to the acceleration of mass diffusion by the flow as follows. The ocp, the equilibrium potential between anodic and cathodic reactions (eqs. (1) and (2)), was shifted by the acceleration of the anodic reaction. The growth of the $Mg(OH)_2$ film was retarded by the diffuse away Mg^{2+} and OH^- ions by the flow, leading to the decrease of the protectiveness of the surface film. Simultaneously, the chemical dissolution of the $Mg(OH)_2$ film might be accelerated by the increase of the rotation speed due to the prevention of the pH increase near the surface. The pH near the surface of the Mg disk at a relatively high rotation speed would be kept at the pH of bulk solution, pH 6, at which the stability of Mg^{2+} is much higher than that of $Mg(OH)_2$.[16]

Interestingly, the surface of the Mg disk immersed at 720 and 1440 rpm for 3.6 s showed no breakdown of the surface film, whereas that of a disk at lower rotation speeds showed breakdown of the surface film, as shown in Fig. 3. Polishing scars and luster remained on the surface of the Mg disk at a relatively high rotation speed. This result indicates that the breakdown of the surface film is retarded by the existence of a flow.

The increase of ocp in the last 600 s of immersion at 0 and 120 rpm was accompanied by the breakdown of the surface film. The filiform corrosion grew along polishing scars on the surface of the Mg disk at 0, 120, and 240 rpm. The induction time for the breakdown of the surface film of the Mg disk in this study was shorter than that of the 3N-Mg and 6N-Mg specimen finished with 1 μm diamond paste.[18] The roughness of the Mg disk finished with #600 SiC paper in this study was larger than that of the specimens finished with diamond paste. The surface roughness seems to affect the initiation of the breakdown of the surface film. The ratio of the breakdown area to the luster area that was not broken down clearly decreased with the increase of the rotation speed. In the case of 0 rpm, almost all the area was broken down and colored black, and a white gel-like corrosion product covered the broken-down surface. This deposited corrosion product probably retarded the diffusion of dissolved metal ions, leading to the increase of ocp in the last 600 s of immersion.

3.3 Polarization curves

Figure 4 shows the polarization curves of the Mg disk at 0, 120, and 1440 rpm subsequently measured after the 3.6 ks immersion. The polarization curves at 240 and 720 rpm were very similar to that at 120 rpm. More than two experiments for every rotation speed were conducted; the cathodic current density (I_{cath}) at −1.8 V (vs. SCE), the corrosion potential (E_{corr}) on the anodic polarization curve, and anodic current density (I_{ano}) at −1.2 V were obtained from the curves and are summarized in Fig. 5.

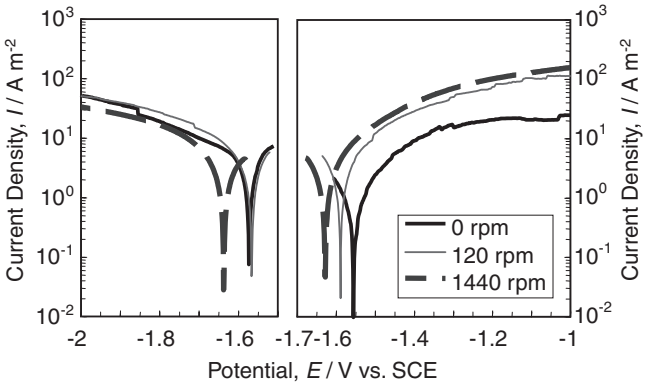

Fig. 4 Polarization curves of a Mg disk at various rotation speeds in a 0.6% NaCl solution.

The I_{cath} abruptly increased with the existence of a flow at 120 rpm and decreased with the increase of the rotation speed up to 240 rpm. Over 240 rpm, the I_{cath} was almost constant with the increase of the rotation speed. The surface film of the Mg disk at 0 rpm was fully broken down during the 3.6 ks immersion before the polarization, as shown in Fig. 3, indicating that the actual surface area increased. On the other hand, the corrosion product covering the surface prevented the diffusion of the H_2O molecule, retarding the cathodic reaction. The surface film of the Mg disk at 120 rpm was partially broken down, whereas the deposited corrosion product was less than that at 0 rpm. This result indicates that the effective surface area for the cathodic reaction on the Mg disk at 120 rpm was larger than that at 0 rpm, causing the higher I_{cath} at 120 rpm than that at 0 rpm. The surface film of the Mg disk over 240 rpm was not significantly broken, indicating that the effective surface area at over 240 rpm was smaller than that at 120 rpm. Thus, the I_{cath} at over 240 rpm was smaller than that at 120 rpm.

The I_{ano} increased with the existence of a flow, indicating the acceleration of the diffusion of the dissolved Mg^{2+} ion by the flow. This result agrees with the decrease of ocp with the existence of a flow, as shown in Fig. 2. On the other hand, the I_{ano} appeared to reach constant levels at over 720 rpm, suggesting that the anodic reaction was limited by the ionization step of Mg at −1.2 V.

The polarization curves at 0 and 120 rpm sometimes showed a stepwise increase of the current density. The stepwise increase on the cathodic and anodic polarization curves probably corresponds to the formation and detachment of the hydrogen gas bubble and the local breakdown of the surface film, respectively.

3.4 Impedance behavior

Figures 6–8 show the change in the impedance behavior of the Mg disk at 0, 120, and 1440 rpm during immersion in a 0.6% NaCl solution for 21.6 ks. In the case of 0 rpm, the phase curve clearly showed a peak between 10^3 and 10^1 Hz,

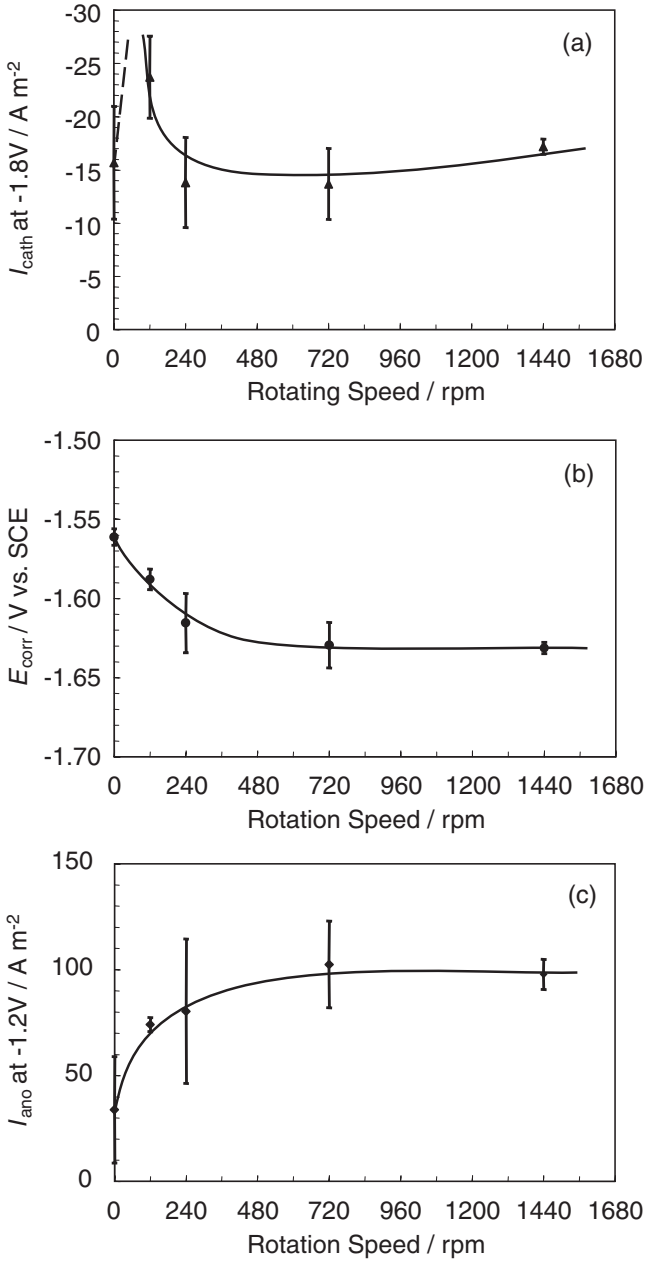

Fig. 5 (a) I_{cath} at -2.0 V, (b) E_{corr}, and (c) I_{ano} at -1.2 V on the polarization curves of a Mg disk as a function of rotation speed in a 0.6% NaCl solution.

indicating the existence of a surface film having a time constant. In the case of 120 and 1440 rpm, the phase curve showed a peak between 10^3 and 10^1 Hz having a shoulder peak at around 1 Hz, indicating a surface film having two time constants. Then, an equivalent circuit having one or two sets of parallel circuits composed of a resistance (R) and a capacitance (C) is suggested for the Mg disk at 0, 120, and 1440 rpm. However, further analysis on the surface structure is necessary to draw an equivalent circuit.

The constant Z value between 10^1 and 10^{-1} Hz was higher than that between 10^{-1} and 10^{-2} Hz, as shown in Figs. 7 and 8, suggesting that the corrosion resistance of a Mg disk corresponds to the constant Z value between 10^1 and 10^{-1} Hz. Then, the difference between two constant Z values at 1 and 10^4 Hz was obtained as a resistance of the surface

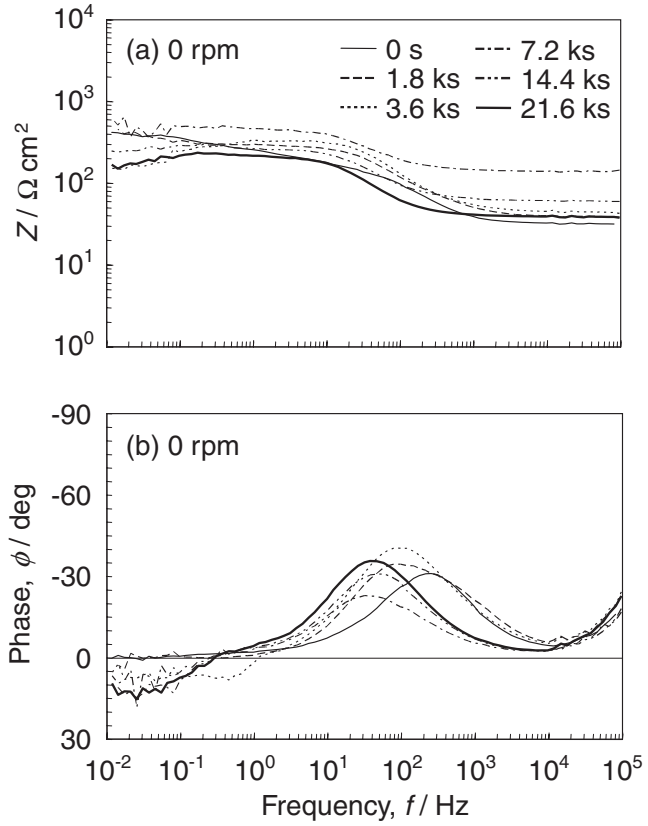

Fig. 6 Changes in Bode plots of a Mg disk at 0 rpm in a 0.6% NaCl solution.

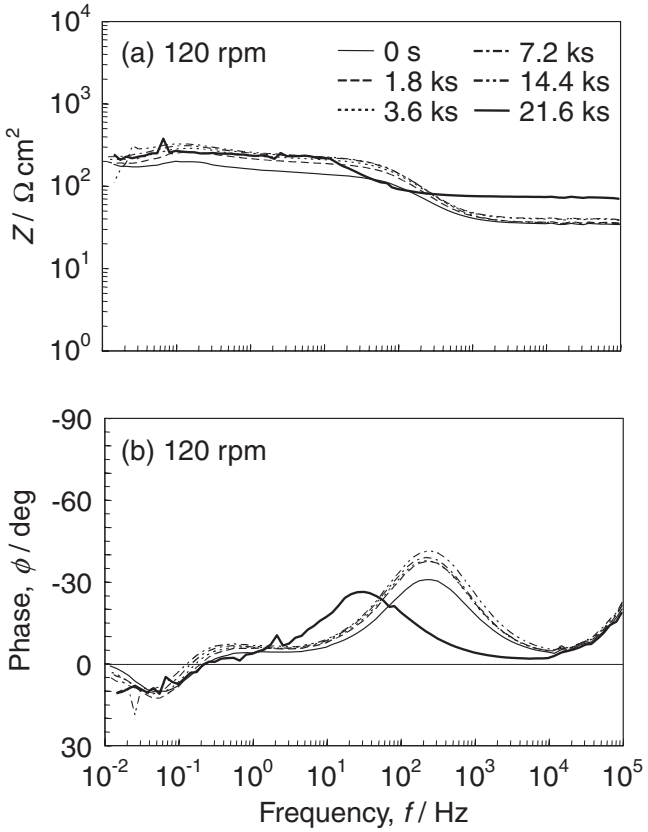

Fig. 7 Changes in Bode plots of a Mg disk at 120 rpm in a 0.6% NaCl solution.

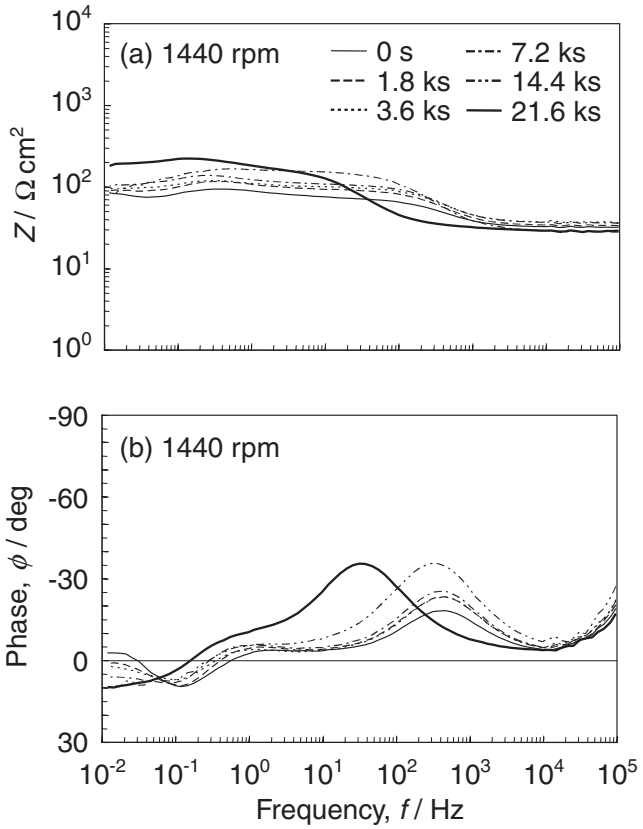

Fig. 8 Changes in Bode plots of a Mg disk at 1440 rpm in a 0.6% NaCl solution.

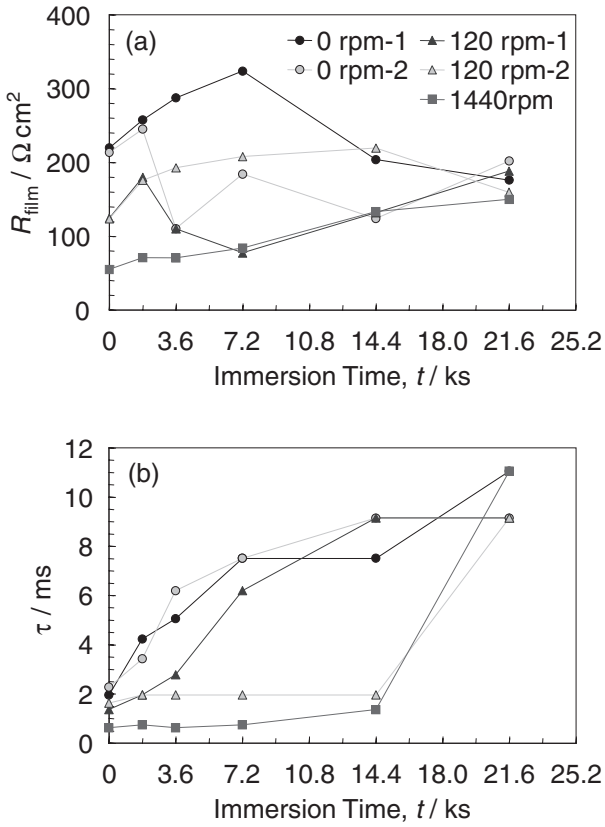

Fig. 9 (a) R_{film} and (b) τ of a Mg disk as a function of the immersion time in a 0.6% NaCl solution at rotation speeds of 0, 120, and 1440 rpm.

film (R_{film}) and is plotted in Fig. 9(a). The time constant ($\tau = R_{film} \cdot C_{dl}$) ($C_{dl}$: capacitance of the double layer) was obtained as a frequency characteristic from the break-point frequency between 10^2 and 10^1 Hz and is plotted in Fig. 9(b). Two transient curves of the R_{film} and τ of the Mg disk at 0 and 120 rpm are plotted in Fig. 9, since the reproducibility of the experiment was poor. The optical images of the Mg disk surface after the 21.6 ks immersion with the impedance measurement are shown in Fig. 10.

The surface of the Mg disk at 0 rpm after the 21.6 ks immersion was covered with filiform corrosion growing along the polishing scar, and large pits also formed along the polishing scar. A gel-like corrosion product preferentially precipitated on the pits. The surface of the Mg disk at 120 rpm was also covered with filiform corrosion, but the filiform corrosion grew along the direction of the rotation flow. The corrosion product accumulated along the edge of the silicone coating, probably because the corrosion product was carried by the solution flow. The surface of the Mg disk at 1440 rpm was partially covered with the filiform corrosion growing along the rotation flow.

Immediately after the immersion, the R_{film} at 0 rpm was higher than that at 120 and 1440 rpm, indicating that the protectiveness of the surface film formed immediately after immersing the Mg disk at 0 rpm was higher than that obtained at 120 and 1440 rpm. The abrupt increase of the pH of a solution near the surface at 0 rpm would encourage the formation of a thick $Mg(OH)_2$ film. The R_{film} of the Mg disk at 0 and 120 rpm increased in the beginning and showed a large fluctuation, sometimes increasing and sometimes decreasing. The fluctuation might correspond to the breakdown of the surface film. This decrease in the 3.6 ks immersion and subsequent increase of impedance of 3N-Mg were reported by Takatani *et al.* in a 0.5N NaCl solution.[19] The R_{film} at 1440 rpm slightly increased during 21.6 ks, indicating that the $Mg(OH)_2$ film grew slightly. On the other hand, the R_{film} values at various rotation speeds reached a similar value at 21.6 ks of immersion, although they followed a different transient, indicating that the corrosion resistance of magnesium depends on the breakdown area of the surface film.

The τ at 0 rpm linearly increased with the increase of the immersion time, suggesting that the diffusivity at the interface decreased during immersion, probably owing to the deposition of the gel-like corrosion product. The τ at 120 rpm sometimes increased and sometimes remained unchanged up to 14.4 ks of immersion. When the τ increased, the R_{film} decreased. Thus, the increase of τ seems to correspond to the breakdown of the surface film. In the case of 1440 rpm, the τ was constant up to 14.4 ks of immersion and subsequently increased between 14.4 and 21.6 ks. The breakdown of the surface film of the Mg disk at 1440 rpm might occur between 14.4 and 21.6 ks.

3.5 Influence of the existence of a flow on the breakdown of surface film

The breakdown of the surface film was prevented by the existence of a flow, as shown in Figs. 3 and 10. Since the breakdown is initiated by the adsorption of the Cl^- ion, the following two mechanisms are assumed to take place. The

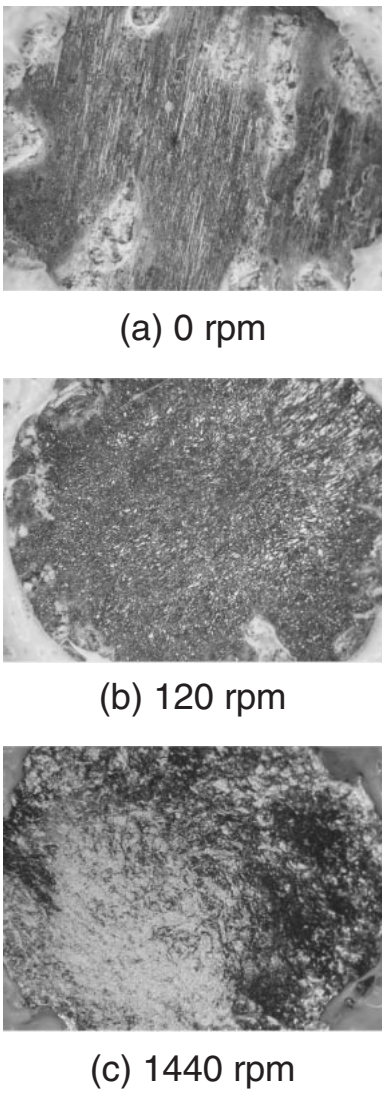

Fig. 10 Images of the surface of a Mg disk immersed at (a) 0 rpm, (b) 120 rpm, and (c) 1440 rpm in a 0.6% NaCl solution for 21.6 ks with impedance measurement.

outermost surface of the $Mg(OH)_2$ film is rapidly dissolved under the flow; thus, the Cl^- ion cannot adsorb on the surface for enough time to break the film. On the other hand, the continuous dissolution of the outermost surface removes the defect of the outermost surface formed by the Cl^- ion before the defect grows into the obvious breakdown of the surface film. The prevention of anion adsorption by the existence of a flow was indicated by the XPS analysis data. Borate was detected on a magnesium surface immersed in a borate buffer solution at 0 rpm; however, the signal originated from the B 1 s electron was under the detection limit on a magnesium surface immersed at 1440 rpm. The details of the surface analysis will be reported in the near future.

4. Conclusion

Polarization and impedance measurements were carried out on a pure Mg disk in a 0.6 mass% NaCl solution using a rotating disk electrode to understand the influence of a controlled flow on the corrosion behavior of magnesium.

The existence of a flow caused the decrease of ocp, the increase of I_{ano} on the polarization curve, and the decrease of R_{film} obtained from the impedance curve, indicating the acceleration of the Mg dissolution and the retardation of the growth of the surface $Mg(OH)_2$ film. Interestingly, the existence of a flow retarded the breakdown of the surface film. After the breakdown of the surface, the R_{film} did not depend on the flow rate. The corrosion rate of magnesium is determined by the breakdown area on the surface. The deposited corrosion product seems to decrease the diffusivity at the interface and retard the corrosion reaction of magnesium.

The implanted bioabsorbable magnesium alloy is exposed to the dynamic environment with a blood flow or the natural convection of body fluid at around neutral pH. To accurately estimate the degradation rate of magnesium and its alloys *in vitro*, the flow rate of the test solution should be controlled depending on the implanted part of the body.

Acknowledgement

We would like to thank Ms. Sanae Sugita for her valuable support of the experiments. This work was supported by a Grant-in-Aid for Young Scientists (B) (18760554).

REFERENCES

1) H. Tanaka: Chemical Review Quarterly **27** (1995) 3–12.
2) G. B. Stroganov, E. M. Savitsky, N. M. Tikhova, V. F. Terekhova, M. V. Volkow, K. M. Sivash and V. S. Borodkin: Magnesium-base alloy for use in bone surgery. US Patent 3687135 (1972).
3) E. D. McBride: J. Am. Med. Assoc. **111** (1938) 2464–2467.
4) C. P. McCord: Indust. Med. **11** (1942) 71–78.
5) J. Hillis: *Magnesium Technology – Metallurgy, Design Data, Applications* –, (Springer, New York, 2006) pp. 469.
6) B. Heublein, R. Rohde, V. Kaese, M. Niemeyer, W. Hartung and A. Haverich: Heart **89** (2003) 651–656.
7) R. Erbel, C. Di Mario, J. Bartunek, J. Bonnier, B. de Bruyne, F. R. Eberli, P. Eme, M. Haude, B. Heublein, M. Horrigan, C. Ilsley, D. Böse, J. Koolen, T. F. Lüscher, N. Weissman and R. Waksman: Lancet **369** (2007) 1869–1875.
8) C. Di Mario, H. Griffiths, O. Goktekin, N. Peeters, J. Verbist, M. Bosiers, K. Deloose, B. Heublein, R. Rohde, V. Kasese, C. Ilsley and R. Erbel: J. Intervent. Cardiol. **17** (2004) 391–395.
9) P. Peeters, M. Bosiers, J. Verbist, K. Deloose and B. Heublein: J. Endovasc. Ther. **12** (2005) 1–5.
10) F. Witte, J. Fischer, J. Nellesen, H.-A. Crastack, V. Kaese, A. Pisch, F. Beckmann and H. Windhagen: Biomaterials **27** (2006) 1013–1018.
11) E. Gulbrandsen: Electrochim. Acta **37**(8) (1992) 1403–1412.
12) J. Lévesque, D. Dubé, M. Fiset and D. Mantovani: Mater. Sci. Forum **426–432** (2003) 521–526.
13) M. Kaibara and A. Sakanishi: *Biorheology*, (Sangyo-tosho, Tokyo, 1999) pp. 78. (in Japanese)
14) M. Sugawara and N. Maeda: *Hemorheology and Blood Flow*, (Corona Publishing, Tokyo, 2003) pp. 75. (in Japanese)
15) G. L. Makar and J. Kruger: Int. Mater. Rev. **38** (1993) 138–153.
16) M. Pourbaix: *Atlas of Electrochemical Equilibria in Aqueous Solutions*, English ed. (National Association of Corrosion Engineers, Texas, 1974) pp. 139–145.
17) G. Wada: Denki-Kagaku (now: Electrochemistry) **25** (1957) 164–165. (in Japanese)
18) N. Hara, Y. Kobayashi, D. Kagaya and N. Akao: Corros. Sci. **49** (2007) 166–175.
19) Y. Takatani, R. Tamai, A. Yamamoto and H. Tsubakino: J. Jpn. Inst. Light Metals **55**(8) (2005) 357–362. (in Japanese)